Model for Energy Transfer in Polymer/Dye Blends Based on Point−Surface Dipole Interaction

J. Cabanillas-Gonzalez,*,† A. M. Fox,‡ J. Hill,‡ and D. D. C. Bradley§

Dipartimento di Fisica, Instituto Nazionale per la Fisica della Materia, Politecnico di Milano, 20133, Milano, Italy, Department of Physics and Astronomy, The University of Sheffield, Hicks Building, Hounsfield Road, Sheffield S3 7RH, United Kingdom, and The Blackett Laboratory, Imperial College London, Prince Consort Road, SW7 2BZ London, United Kingdom

Received March 1, 2004. Revised Manuscript Received June 15, 2004

We report a new model for the Förster energy transfer in blends of Nile Red dye in poly(9,9-dioctylfluorene) (PFO). We base our discussion on the possible arrangement of the dye molecules distributed in domains surrounded by polymer. These geometric considerations lead to a R^{-3} functional dependence for the energy transfer, different from the R^{-6} deduced by Förster for pointlike dipole−dipole interaction. The experimental value found for the Förster radius, namely 3.2 nm, is in good agreement with 3.6 nm obtained from the spectral overlap of donor emission and acceptor absorption.

I. Introduction

The Förster energy transfer mechanism in blends of conjugated materials is currently exploited for the design of organic light-emitting diodes.[1−3] Suitable combinations of host−guest organic materials can be employed to efficiently tune the emission toward different parts of the visible spectrum. The efficiency of this process in certain blends is such that total transfer can be achieved even at a very low concentration of guest molecules.[4,5] This is mostly due to the shorter donor−acceptor distances achieved in blends than in multilayer structures and the dramatic dependence of the energy transfer rate with the average donor−acceptor separation R predicted by the Förster theory:[6]

$$k_{ET} = \frac{1}{\tau_o}\left(\frac{R_o}{R}\right)^6 \qquad (1)$$

where τ_o is the donor radiative lifetime and R_o is the Förster radius defined as the distance for which direct donor decay is equally likely to transfer energy to the acceptor. There are, however, several reports in the literature concerning energy transfer in polymer−polymer or polymer−dye blends which suggest discrepancies with the Förster theory.[4,5,7] This deviation is partly due to the fact that the R^{-6} dependence arises from considerations of the dipole−dipole interaction between two isolated molecules. This type of molecule−molecule interaction is unlikely to take place in polymer blends since the donor groups are not isolated but distributed along polymer chains. At the same time, the polymer chains may be arranged forming *bulky solids* (we refer to them as *surfaces*) where the acceptor molecules are embedded. A more appropriate description should take into account not only point−point dipole interactions but also point−surface or surface−surface interactions. These different types of interactions lead to variations of the functional dependences in eq 1 as Hill et al. demonstrated.[8,9] In their work they studied energy transfer between two LB films of PFO and poly(9,9-dioctylfluorene-*co*-benzothiadiazole) (BT) obtaining an energy transfer dependence $K_{ET} \alpha R^{-2}$ which is in agreement with the extension of the van der Waals potential energy between two surfaces. In polymer/polymer blends however, the difficulty arises from the random distribution of the donor and acceptor chromophores in the blend. Hence, to estimate the average donor−acceptor separation becomes extremely complicated. Alternatively, polymer/dye blends offer a simplified insight to the problem: dye molecules blended in polymer can be considered as pointlike dipoles spatially fixed which interact with the *surrounding walls* of polymer chromophores. Accordingly, we have assessed the Förster law for the energy transfer in blends of poly(9,9-dioctylfluorene) and Nile Red. Nile Red is a laser dye with high photoluminescence quantum efficiency (PLQE) in solution (78% in acetonitrile)[10] and good red emission color ((0.64, 0.34) CIE coordinates[11]). Concern-

* To whom correspondence should be addressed. E-mail: juan.cabanillas@polimi.it.
† Politecnico di Milano.
‡ The University of Sheffield.
§ Imperial College London.

(1) Tasch, S.; Brandstäter, C.; Meghdadi, F.; Leising, G.; Froyer, G.; Athouel, L. *Adv. Mater.* **1997**, *9*, 33.
(2) Berggren, M.; Dodabalapur, A.; Slusher, R. E.; Bao, Z. *Nature* **1997**, *389*, 466.
(3) Greenham, N. C.; Moratti, S. C.; Bradley, D. D. C.; Friend, R. H.; Holmes, A. B. *Nature* **1993**, *365*, 628.
(4) Buckley, A. R.; Rahn, M. D.; Hill, J.; Cabanillas-Gonzalez, J.; Fox, A. M.; Bradley, D. D. C. *Chem. Phys. Lett.* **2001**, *339*, 331.
(5) Virgili, T.; Lidzey, D. G.; Bradley, D. D. C. *Adv. Mater.* **2000**, *12*, 58.
(6) Förster, T. *Ann. Phys.* **1948**, *2*, 55.
(7) Cerullo, G.; Stagira, S.; Zavelani-Rossi, M.; De Silvestri, S.; Virgili, T.; Lidzey, D. G.; Bradley, D. D. C. *Chem. Phys. Lett.* **2001**, *335*, 27.
(8) Hill, J.; Buckley, A. R.; Rahn, M. D.; Heriot, S. Y.; Worsfold, O.; Fox, A. M.; Richardson, T. H.; Cabanillas-Gonzalez, J.; Bradley, D. D. C. Proceedings of Conference on Lasers and Optoelectronics. *OSA Technical Digest* **2002**, *73*, 492.
(9) Hill, J.; Heriot, S. Y.; Worsfold, O.; Richardson, T. H.; Fox, A. M.; Bradley, D. D. C. *Synth. Met.* **2003**, *139* (3), 787.

10.1021/cm0496669 CCC: $27.50
Published on Web 09/25/2004

ing its application in emissive devices, there have been reports on Nile Red lasing,[12] and LED design either in multilayer structures or blended in polymer.[13,14] The moderate spectral overlap between PFO emission and Nile Red absorption (R_o = 3.6 nm calculated from spectral overlap[11]) guarantees the establishment of an energy transfer mechanism in the blend. We have performed steady state and time-resolved photoluminescence (PL) measurements on blends with different concentrations of Nile Red. The dependence of the energy transfer rates on the average donor−acceptor separation was obtained and compared with the functional dependence predicted by Förster for pointlike dipole−dipole interaction. We discuss the results in terms of geometrical arrangement of the donor chromophores that involve the acceptor dipoles.

II. Experimental Details

Nile Red purchased from Aldrich was dispersed in PFO by blending two master tethrahydrofuran solutions of polymer and dye in the required ratios. The concentration of polymer in solution (15 g/L) was kept constant. Spin-coating of blend solutions at 1500 rpm produced films with a typical thickness of approximately 100 nm. PLQE measurements were carried out using a 354 nm He−Cd laser as the excitation source with a typical output power below 1 mW/cm^2. Films were placed inside an integrating sphere (coated uniformly with a reflecting material) in a N_2 atmosphere to avoid photooxidation. An optic fiber coupled to a Spex 270M scanning monochromator with a photomultiplier detector was used to separate the light into its different wavelength components. PLQE values of PFO and Nile Red in blends were calculated by integrating the PL emission corresponding to PFO (400−510 nm) and Nile Red (510−700 nm), respectively, and normalizing it by the light absorbed by the sample. PL dynamics of the donor were monitored at 450 nm using the second harmonic of a 780 nm mode-locked Spectra Physics Ti:Sapphire laser delivering pulses of 150 fs. A spectrum analyzer was used to monitor the profile of the pulses. PL from the sample was collected in reflection geometry and sent onto a subtractive double monochromator. The emission was resolved in time with a 600 fs Hadland streak camera. Analysis of the image was obtained using custom software designed for the streak camera and which allows the averaging of intensity in selected intervals of time.

III. Results

Absorption and PL spectra of Nile Red blended in an inert matrix of poly(methyl methacrylate) (PMMA) are depicted in Figure 1a and b, respectively. Figure 1a displays the absorption of four films with different Nile Red/PMMA weight ratios. A broad absorption band with a maximum at 532 nm dominates the spectra. Besides this, a shoulder is visible at around 555 nm for the most concentrated 10:100 blend film. The PL spectra of Nile Red displayed in Figure 1b show a progressive redshift as the content of Nile Red in PMMA is increased. In addition to this, the shape of the spectra undergoes a

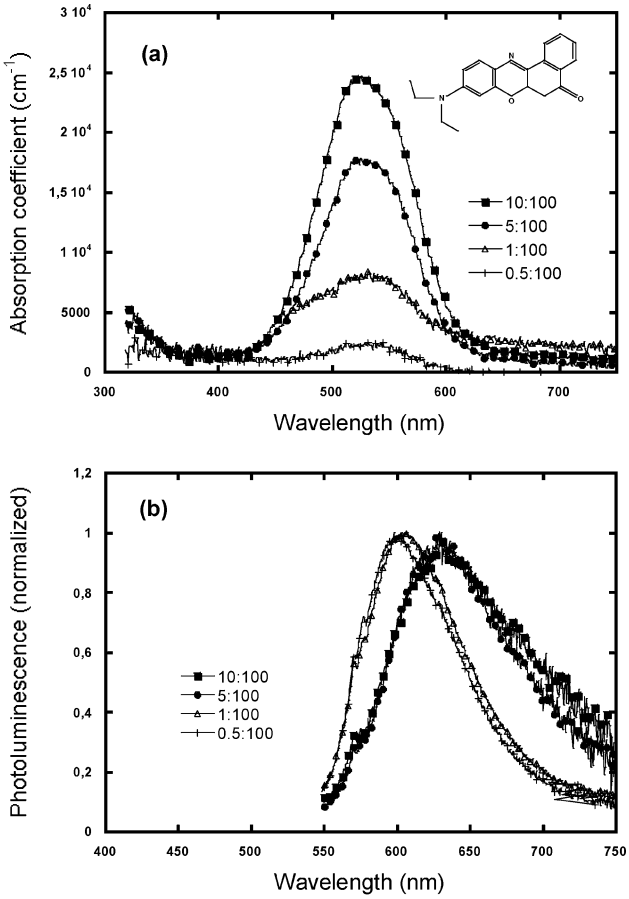

Figure 1. (a) Absorption spectra of Nile Red blended at different concentrations with PMMA. The vertical shift of the spectra is the result of scattering. The chemical structure is displayed in the inset. (b) Normalized photoluminescence spectra of Nile Red in PMMA.

significant change. Meanwhile the PL spectrum of the 0.5:100 film is composed of a band centered at 598 nm with a long tail, and the 10:100 film exhibits a broad PL band located at 630 nm. The absorption spectra of Nile Red/PFO blends and pure PFO are shown in Figure 2. The absorption of Nile Red in the region around the maximum absorption of pure PFO (390 nm) is negligible. This allows us to exclude the possibility of direct excitation when pumping at 390 nm and therefore facilitates the identification of energy transfer from PFO to Nile Red. Concerning the spectra of blends, their shape is a superposition of the pure materials spectra. Flattening of PFO maximum absorption at 390 nm is characteristic of thick films with rough topographies.[15] The concentration dependence of the absorption coefficient at 530 nm which corresponds to the maximum absorption of Nile Red is displayed in the inset of Figure 2. A deviation from the linear behavior takes place over weight ratios of 1:100, which suggests the presence of Nile Red aggregates in the film in this concentration regime. Similar observations are often reported in small molecules with aromatic structures.[16,17] Figure 3 depicts

(10) Camargo Dias, L.; Custodio, R.; Pessine, F. B. T. *Chem. Phys. Lett*. **1999**, *302*, 505.
(11) Cabanillas-Gonzalez, J. Ph.D. Thesis, Imperial College, London, 2003.
(12) Kuwata-Gonokami, M.; Takeda, K.; Yasuda, H.; Ema, K. *Jpn. J. Appl. Phys.* **1992**, *31*, 99.
(13) Kusano, H.; Hosaka, S.; Shiraishi, N.; Kawakami, S.; Sugioka, K.; Kitagawa, M.; Ichino, K.; Kobayashi, H. *Synth. Met*. **1997**, *91*, 337.
(14) Nakamura, A.; Tada, T.; Mizukami, M.; Hirose, S.; Yagyu, S. *Appl. Phys. Lett.* **2002**, *80*, 2189.
(15) Ariu, M.; Lidzey, D. G.; Bradley, D. D. C. *Synth. Met*. **2000**, *111*, 607.
(16) Matoussi, H.; Murata, H.; Merrit, C. D.; Iizumi, Y.; Kido, J.; Kafafi, Z. H. *J. Appl. Phys*. **1999**, *86* (5), 2642.
(17) List, E. J. W.; Holzer, L.; Tasch, S.; Leising, G.; Castellani, M.; Luzzati, S. *Opt. Mater.* **1999**, *12* (2−3), 311.

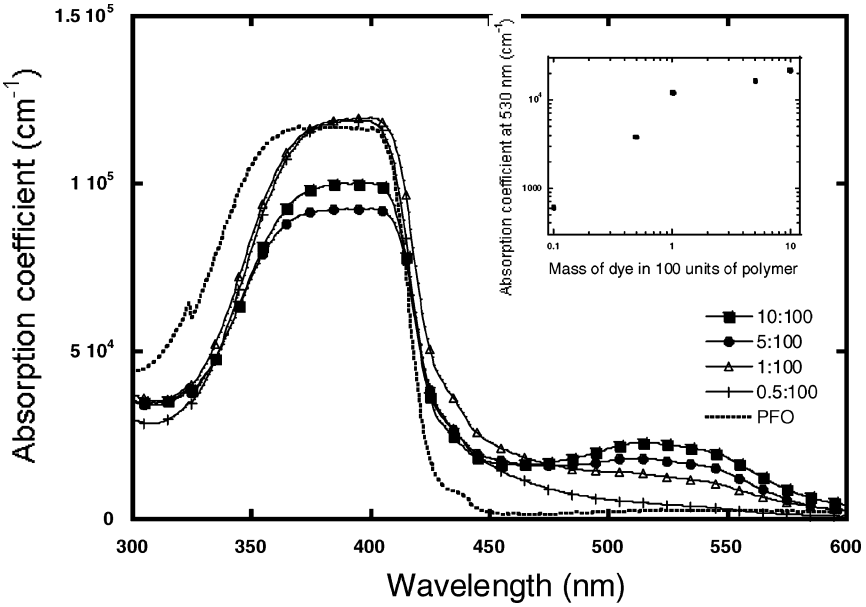

Figure 2. Absorption spectra of blends of 10:100 (squares), 5:100 (circles), 1:100 (triangles), and 0.5:100, (crosses) dye/polymer weight ratio and pure PFO (dotted). The inset figure represents the absorption coefficient at 530 nm vs. Nile Red concentration.

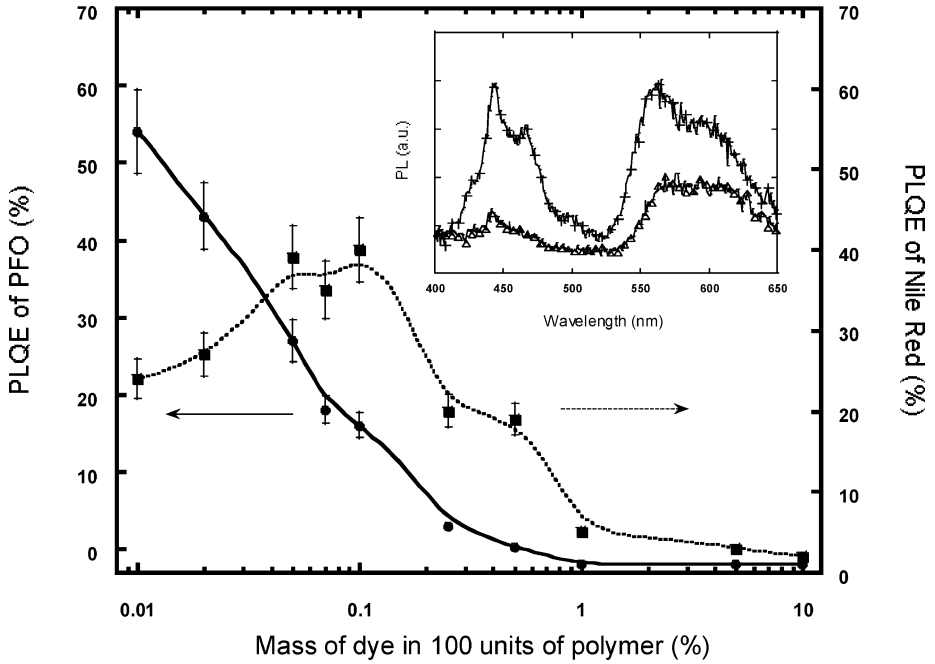

Figure 3. PLQE values of PFO (circles) and Nile Red (squares) in blends with different dye concentrations. The values of pure PFO and Nile Red dispersed in PMMA were 57% and 51%, respectively. The PL spectra in the inset correspond to 0.07:100 (crosses) and 0.5:100 (triangles) blends. These two are located in different concentration regimes: increase of Nile Red efficiency, and decrease, respectively. Note that the drop in efficiency is accompanied by a redshift of the PL spectrum.

the PLQE values of PFO and Nile Red in blends with different dye contents. As the doping concentration rises, PFO emission quenches and the PLQE values of Nile Red experience an improvement. These two orthogonal behaviors constitute a clear proof for energy transfer of excitations from the polymer to the dye. The rise in Nile Red PLQE saturates at 0.1:100 weight ratio after reaching a value of 40%. At this concentration value PFO emission is not completely extinguished yet (16% at 0.1:100 weight ratio) so that total transfer is not fully achieved. As the doping is increased further, the efficiency of the dye drops and the PL spectra undergo a broadening and loss of features likely associated with the formation of dye−complex species with low quantum yield (inset of Figure 3). It is remarkable that these PL changes have no correspondence in the absorption spectra. This fact is often presented as a proof for formation of excimers, species characterized by broad emission and low PL quantum yields.[5,18] PL decay curves of PFO in blends are shown in Figure 4. The decay curves were fitted to single exponentials with fairly good agreement: there were only slight deviations in the more heavily doped 5:100 and 10:100 samples. The increased noise observed in these two curves results from the low PFO emission intensity due to the high percentage of PFO excitons that are quenched, as shown

(18) Conwell, E. *Synth. Met.* **1997**, *86*, 1.

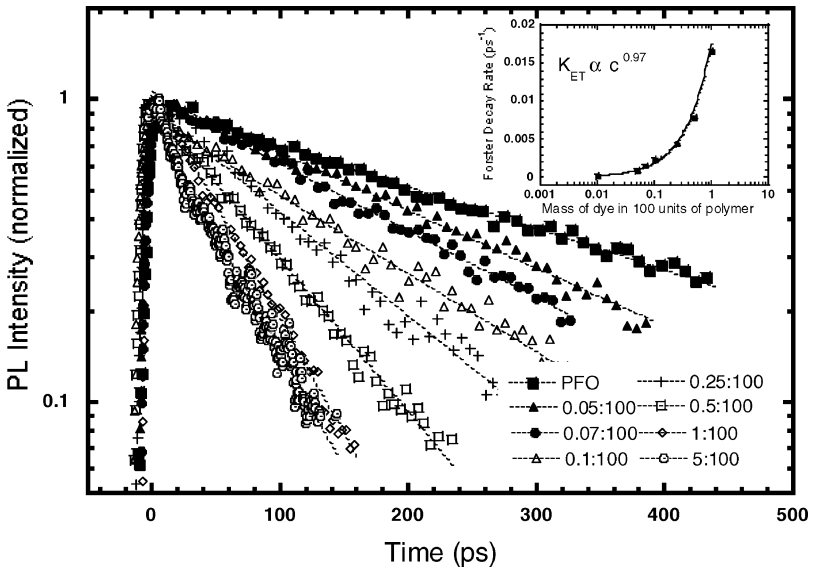

Figure 4. Log−lin plot of the PFO PL decay excited at 390 nm for a range of blends. The emission was detected at 450 nm. The inset figure displays the dependence of the energy transfer rate with the dye content.

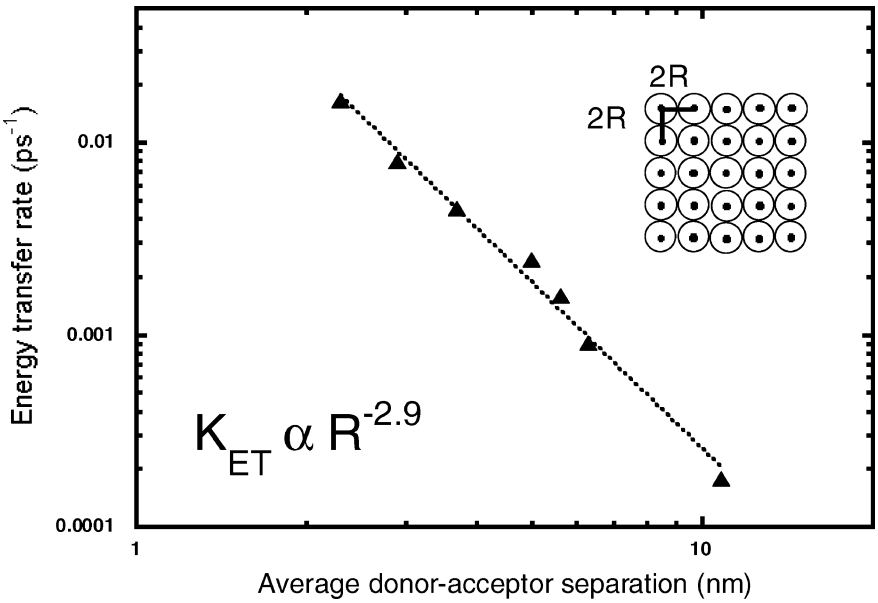

Figure 5. Log−log plot of the dependence of the energy transfer rate on the average donor−acceptor distance. The inset figure shows the hard sphere distribution, which considers the molecules centered in a sphere of volume $(4/3)\pi R^3$, being the average distance between two molecules $2R$.

by the PLQE data. An acceleration of PFO dynamics is detected as the concentration of dye in blends is increased. The energy transfer rates were deduced by subtracting the decay rate of pure PFO ($K_{PFO} = 2.5 \times 10^{-3}$ ps^{-1}) from the total decay rate of blends calculated from the parameters of the fit. The dependence of the Förster rates with the dye concentration follows a power law with an exponent of nearly one (0.97) (inset of Figure 4) showing a clear enhancement of energy transfer rate as the Nile Red concentration is increased.

IV. Discussion

Assuming that the Nile Red molecules are embedded in the matrix occupying each molecule the volume of a hard sphere (inset of Figure 5), the dye concentration will be related to the average intermolecular distance $2R$ as $c\alpha R^{-3}$. According to the concentration dependence of the energy transfer rate $k_{ET}\alpha c$ found in the last paragraph we infer that the energy transfer rates follow a law of the type $k_{ET}\alpha R^{-3}$, as it is depicted in Figure 5. This functional dependence represents a clear deviation from the R^{-6} law described for point−point dipole interactions. Additional proof for the deviation of the experimental data from the predictions of the standard Förster model is provided in Figure 6. According to the standard Förster model the dependence of the donor PLQE with the acceptor concetration is given by[6]

$$\frac{\phi}{\phi_o} = 1 - \pi^{1/2}\gamma \exp(\gamma^2)(1 - erf\gamma) \text{ with } erf\gamma = 2\pi^{-1/2}\int_0^{\gamma}\exp(-x^2)dx \quad (2)$$

where ϕ_o is the fluorescence of pure PFO and γ holds for the molar concentration of acceptor related to the

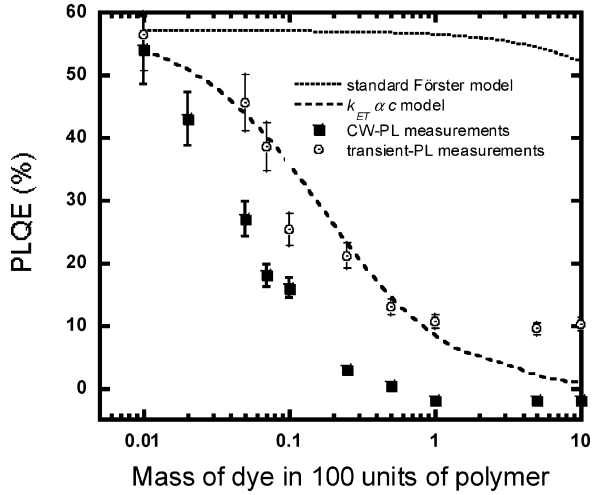

Figure 6. Comparison between the PLQE values obtained experimentally with those predicted theoretically from the standard Förster model (dotted line) and the proposed $k_{ET}\alpha c$ approximation (dashed line). The experimental PLQE values were calculated from steady state (filled squares), and transient PL measurements (open circles). The error associated with the PLQE measurement was estimated as 10% of the absolute value.

critical molar concentration given by:

$$\gamma_c = \frac{3000}{2\pi^{3/2} N_A R_o^3} \tag{3}$$

where N_A and R_o holds for the Avogadro's number and Förster radius, respectively. For our purposes we have employed the Förster radius of 3.6 nm calculated from spectral overlap of donor emission and acceptor absorption. A comparison of the theoretical predictions with the experimental values is displayed in Figure 6. Two types of experimental data sets were employed: PLQE values obtained from CW−PL measurements and from transient−PL measurements. To calculate the PLQE values from the PL decay curves we have applied the expression for the Stern−Volmer kinetics, which predicts a relation between the PLQE (ϕ) and energy transfer rate given by

$$\frac{\phi}{\phi_o} = 1 - \frac{k_{YM}[^1Y]}{k_M + k_{YM}[^1Y]} \tag{4}$$

where ϕ_o is the PLQE value of pure PFO (57%), $k_{YM}[^1Y]$ is the rate of energy transfer from the singlet donor ^1M to the singlet acceptor ^1Y which depends on the acceptor concentration $[^1Y]$, and k_M is the decay rate of ^1M singlets. Substitution of k_{YM} by the transfer rates calculated from the PL decay curves provides the PLQE values of PFO at each concentration. At first glance, the PLQE values obtained from CW−PL measurements show a larger degree of quenching than those predicted from lifetime measurements. Here we should remark that energy transfer in polymer-based blends proceeds mainly mediated via random exciton diffusion along the polymer chains.[19] This mobile nature of the excitons in conjugated polymers results in a reduction of the donor−acceptor separation, leading therefore to a more efficient transfer as stated by eq 1. Alternatively, transient-PL measurements allow direct monitoring of the donor−acceptor interaction, providing therefore an estimation of the transfer rates, which approaches the values predicted when donor and acceptor dipoles are considered spatially fixed.

Comparison between experimental PLQE values and the predictions of the Förster standard model show a clear lack of agreement. These discrepances are partly motivated by the fact that the standard expression does not take into account energy transfer between PFO chromophores, which it has been mentioned already plays an important role in the case of polymer blends. Alternatively, substitution of k_{ET} in the Stern−Volmer relation by a expression of the type $k_{ET}\alpha c$ provides a fairly good approximation to the experimental data and confirms the validity of the $k_{ET}\alpha R^{-3}$ dependence found from transient-PL measurements. Slight deviation is observed only for the two more concentrated samples, 5:100 and 10:100. These discrepancies could be motivated by the non-exponential PL decay curves exhibited by these two samples. Moreover, we should remark that in the high concentration regime the short donor−acceptor separation provided is likely to induce an increase of static energy transfer with respect to energy migration, leading to a deviation from the predictions of the Stern−Volmer kinetics.

Our experimental observations seem therefore to suggest that the Förster energy transfer interaction represented by eq 1 is not the most suitable model to describe energy transfer in polymer/dye blends. This model considers the donor−acceptor interaction as that between two pointlike dipoles. The probability that each acceptor dipole interacts only with one donor dipole does not seem however to be the more likely situation attending to the large density of donor chromophores photogenerated in its surroundings. A more plausible scenario seems to be instead energy transfer mediated via the interaction between point acceptor dipole and surface or volume distributions of donor dipoles which are located in the neighborhood of the guest molecule.

The expression for a point−surface interaction for a generic attractive potential $-C/R^6$ is $-C\pi\rho/6R^3$ where ρ is the density of interacting groups included in the solid.[20] Hence, the extension of eq 1 to point−surface interaction is given by

$$K_{ET} = \frac{\bar{R}_o^3}{\tau_o R^3} \tag{5}$$

$$\text{with } \bar{R}_o^3 = \frac{\pi\rho R_o^6}{6} \tag{6}$$

where $\bar{R}_o$ is the Förster radius for the molecule-surface interaction, τ_o is the fluorescence lifetime of pure PFO (400 ps), and ρ is in this case the donor chromophore density. The relation between the Förster radius for molecule−molecule and molecule−surface interaction (R_o and $\bar{R}_o$, respectively) is provided by eq 6. There is

(19) List, E. J. W.; Creely, C.; Leising, G.; Schulte, N.; Schluter, A. D.; Scherf, U.; Mullen, K.; Graupner, W. *Chem. Phys. Lett.* **2000**, *325* (1−3), 132.

(20) Israelachvili, J. N. *Intermolecular and Surface Forces*; Academic Press, New York, 1985.

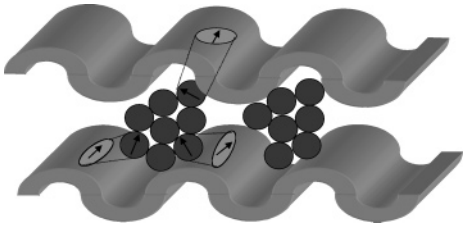

Figure 7. Proposed energy transfer scenario in Nile Red/PFO blends. Two aggregates (represented by clustered spheres), appear embedded between two polymer planes. The chromophore groups in the PFO chains (arrows enclosed in ovals) interact only with the nearest acceptor dipoles (arrows enclosed in circles) due to partial screening of the more distant dipoles contained in the aggregate.

still, however, an issue to be addressed at this point: the assumption that the dye is well-dispersed in the matrix. We have mentioned already the likely presence of dye aggregation phenomena in the bulk. The good dispersion assumption would lead to a situation of each monomer of Nile Red surrounded by the matrix of PFO. This situation would imply interaction with all the solid planes involving the molecule. On the other hand, in the case of dye monomers that form clusters, the surrounding interaction could be partially screened by the rest of the monomers that are present in the cluster, so that each acceptor would interact only with the plane that "is visible for him" as it is depicted in Figure 7. Equation 5 deduced for an interaction between a molecule and a single surface describes therefore better the energy transfer process in the case of acceptor molecules that are clustered.

Finally, we have attempted to estimate R_o from the fitting parameters deduced from Figure 5. The main problem here appears to be how to obtain a value for the density of chromophores (ρ) since different types of chain packing can be found in a spin-coated film. Considerations about the arrangement of the chains are therefore difficult to confirm. Another approach was followed by Lieser et al. They reported a density value of 0.996 g/cm^3 in a related polyfluorene structure ($PF_{2/6}$).[21] This value was based on the observation of a film of polymer sinking in 2-propanol ($\rho = 0.979$ g/cm^{-3}) at room temperature. From the molecular weight of one PFO monomer ($M = 388$ g/mol) we obtain a monomer density value of 1.55 monomers nm^{-3}. Assuming the extension of a chromophore equal to approximately 12 monomer units (proposed by Klärner et al. for poly(dihexylfluorene)[22]) this gives a chromophore density value of $\rho = 0.14$ nm^{-3}. From the fitting parameters of Figure 5 and eq 5 we obtain a point−surface Förster radius of $\bar{R}_o = 4.2$ nm. Substituting $\bar{R}_o$ and ρ in eq 6 produces a final value for R_o of 3.2 nm which is in good agreement with the 3.6 nm obtained from the spectral overlap of the donor emission and acceptor absorption.

V. Conclusion

Förster energy transfer from poly(9,9-dioctylfluorene) to Nile Red has been assessed by making use of a model that considers the Nile Red molecules homogeneously distributed in the bulk, each occupying the volume of a hard sphere. This approximation leads to a dependence on the donor−acceptor separation $K_{ET} \alpha R^{-3}$ which differs significantly from the point−point dipole interaction described by $K_{ET} \alpha R^{-6}$. This R^{-3} dependence is, however, in agreement with the expression expected for a dipole−surface van der Waals type interaction. The good agreement found provides an indication that the Nile Red molecules may be aggregated in the bulk. This hypothesis is supported by the deviation of Nile Red absorption coefficient in blends over 0.5:100 weight ratios from the linear behavior predicted by the Beer−Lambert law. We have shown from a geometric argument that clustering of Nile Red may lead to a screening of surface dipole interactions surrounding the cluster, leading to an effective point−single surface interaction. We estimate from our model a Förster radius R_o of 3.2 nm comparable with the 3.6 nm obtained from the spectral overlap of donor emission and acceptor absorption.

Acknowledgment. We are indebted to The Dow Chemical Company for providing PFO. J.C.-G. is grateful to J. M. Pedrosa and L. Lüer for fruitful discussions.

CM0496669

(21) Lieser, G.; Oda, M.; Miteva, T.; Meisel, A.; Nothofer, H.; Scherf, U.; Neher, D. *Macromolecules* **2000**, *33*, 4490.

(22) Klärner, G.; Miller, R. D. *Macromolecules* **1998**, *31*, 2007.